Ferrite Assisted Geometry-Conformal Magnetic Induction Antenna and Subsea Communications for AUVs

Debing Wei*, Li Yan*, Xuanheng Li†, Jie Wang‡, Jiefu Chen*, Miao Pan*, and Yahong Rosa Zheng§
*Department of Electrical and Computer Engineering, University of Houston, Houston, TX 77204
†School of Information and Communication Engineering, Dalian University of Technology, Dalian, China 116023
‡School of Information Science and Technology, Dalian Maritime University, Dalian, China116026
§Department of Electrical and Computer Engineering, Missouri University of Science and Technology, Rolla, MO 65409

***Abstract*—This paper designs a novel geometry-conformal antenna for Magnetic Induction (MI)-based subsea wireless communications for autonomous underwater vehicles (AUV). The designed tri-directional antennas can be wrapped directly on the surface of AUVs, such that the AUVs fluid dynamics are well maintained to ensure power efficiency of the vehicles. In addition, ferrite materials are added between the MI antenna and the metallic body surface of the AUVs to overcome the shielding effect and enhance the MI signal strength. The designed MI communication system is implemented in hardware and the effectiveness of the geometry-conformal MI antenna is demonstrated through COMSOL simulations and lab experiments.**

I. Introduction

The ocean covers more than 70% of the planet's surface. However, almost 95% of the subsea world is still unexplored. Although researchers can deploy sensor networks in the mysterious subsea world, one of the key challenges is how to collect these valuable data. Since wireless links are preferred to wire links in subsea environments, traditionally, we can either choose EM waves or acoustic waves for subsea data transmission. Unfortunately, neither of them can fulfill the reliable and large data transmission requirements. In view of the fact that EM waves attenuate so fast it is barely useful in sea water [1]. Acoustic waves also suffer from large propagation delay, limited bandwidth, poor channel quality, etc [2], [3], such that the acoustic communication can only support low data rate transmissions (tens of kbps for ranges within 1 km).

Recently, Magnetic Induction (MI) wireless communications are considered to be a great alternative for RF challenging environments such as underground [4] and underwater [5]. MI techniques can support much higher data transmission rates than acoustic techniques due to the much higher operating frequency and much better channel conditions. Particularly, MI techniques work on hundreds of KHz to several MHz with small coil antennas. The information is transmitted through the magnetic field that generated by the current loop in a coil antenna. Since the system is working under resonance conditions, only the modulated signal can be received. Hence, the signal to noise ratio on the receiver side can be significantly improved. In addition, the impacts of multi-path fading can be ignored within the limited communication range (few meters) of MI, thanks to the fast attenuation of magnetic field in lossy medium e.g. sea water.

One of the possible submarine applications for MI is to provide short range wireless communication links between different submarine devices such as AUVs and underwater sensor nodes. Assisted by MI, AUVs can fulfill different tasks more efficiently, including oceanographic surveys and data collection in marine environments.

However, installing a MI antenna on an AUV is challenging. Since MI channel conditions can be significantly influenced by the metallic body of an AUV, the specific MI antenna should be carefully designed. Consequently, the MI channel model should be reevaluated.

In [6], [7], [8], the MI channel model is developed for a two coil antenna system. In [9], the MI channel model is extended for tri-directional coil antennas. However, none of these works take into account the shielding effect of metallic materials. Ahmed *et. al* [10] study the effects of metal structures on MI signal intensity. But in that paper, the metal is placed in between or nearby the coil antennas which is completely different from AUV applications. For a geometry-conformal antenna, the coil is wrapped along the surface of an AUV. Due to the strong shielding effect of metallic surfaces, the magnetic signal is undetectable inside the AUV. Furthermore, installing a coil antenna right above an AUV is also not a wise strategy. Not only can the coil antenna be easily destroyed by the harsh subsea environments, but the fluid dynamic efficiency of an AUV would be ruined by the antenna as shown in Fig.1(a).

To tackle this problem, we design a novel geometry-conformal MI antenna which is directly wrapped along the surface of an AUV. Compared with the conventional triaxial MI antenna in a sphere-like shape attached to the vehicle, this new design has a much better underwater mobility and fluid dynamic efficient as shown in Fig.1(b).

This work was supported in part by the U.S. National Science Foundation under grants US CNS-1343361, CNS-1350230 (CAREER), CNS-1646607, CNS-1702850, CNS-1801925, the National Natural Science Foundation of China under grant 61671102, and the Fundamental Research Funds for the Central Universities under grant No. 3132018294.

978-1-5386-4727-1/18/$31.00 ©2018 IEEE

Although the geometry-conformal antenna design is good for fluid dynamic efficiency, it can not directly be used for transmitting or receiving MI signals, because the metallic surface of an AUV will generate opposite image currents to cancel MI signals. Fortunately, ferrite materials with high magnetic permeability can help to overcome such a problem. As shown in [11], ferrite materials have been used to solve a similar problem on oil pipes for wireless power transfer. In this work, a ferrite assisted geometry-conformal antenna is designed and analyzed in terms of basic communication metrics, i.e, signal to noise ratio, channel capacity and communication range. Our salient contributions are summarized as follows.

- The impacts of the metallic body of an AUV to the magnetic field are analyzed through COMSOL Multiphysics simulations.
- We design a novel ferrite assisted geometry-conformal antenna that can be directly installed on the surface of an AUV. Moreover, the impact of different ferrite parameters, i.e. permeability and coverage angle, on the intensity of magnetic field are fully studied.
- Based on the proposed geometry-conformal antenna, the practical communication range and MI channel capacity under different operation frequencies for submarine applications are obtained.

The rest of this paper is organized as follows. The influence of the metallic body of an AUV to the MI channel is analyzed in Section II. Section III investigates the impact of ferrite materials with different permeability and coverage ratios to the MI signal strength through COMSOL simulations. Based on COMSOL simulation results, the subsea MI channel characteristics, i.e. transmission range and channel capacity, between two geometry-conformal antennas are estimated in section IV. Finally, we conclude the paper in section V.

II. The Influence of the Metallic Body of an AUV to the MI Channel

In this section, the equivalent model of two geometry-conformal antennas is first presented. Then, the magnetic field generated by the transmitter and the induced voltage in the receiver are derived. Lastly, the field model is verified by COMSOL simulation results.

A. Equivalent Model of Two Geometry-Conformal Antennas

For simplicity, the system model of geometry-conformal antenna can be equivalent to a metallic pipe surrounded by two coils as shown in Fig. 2.

The outer radius of the pipe is a and the radius of the loop antenna is b. The pipe is made of metal with conductivity σ and relative permeability μ_r. Assume that the surface of the pipe can be approximated as an impedance defined by

$$Z_s = R_s\left(1+j\right), \tag{1}$$

where $R_s = \frac{1}{\sigma\delta}$, $\delta = \sqrt{\frac{2}{\omega\mu_0\mu_r\sigma}}$, δ represents the skin depth.

B. Fields Generated by Geometric-Conformal Antenna

Because the current is uniform, the field produced will be purely TE$_z$. Correspondingly, the electric vector potential F_z may be written as the sum of an incident potential F_z^i and a scattered potential F_z^s.

$$F_z = F_z^i + F_z^s, \tag{2}$$

where F_z^i is the potential of the current loop in free space and F_z^s is due to the currents induced on the pipe. These vector potentials have the form of

$$F_{z1}^i = \frac{1}{2\pi}\int_{-\infty}^{\infty} A\left(k_z\right) J_0\left(k_\rho\rho\right) e^{-jk_z z} dk_z, \quad \rho < b, \tag{3a}$$

$$F_{z2}^i = \frac{1}{2\pi}\int_{-\infty}^{\infty} B\left(k_z\right) H_0^{(2)}\left(k_\rho\rho\right) e^{-jk_z z} dk_z, \quad \rho > b, \tag{3b}$$

$$F_z^s = \frac{1}{2\pi}\int_{-\infty}^{\infty} C\left(k_z\right) H_0^{(2)}\left(k_\rho\rho\right) e^{-jk_z z} dk_z, \quad \rho > a, \tag{3c}$$

where $k_\rho = (k_0^2 + k_z^2)^{\frac{1}{2}}$, and $k_0 = \omega\sqrt{\mu_0\epsilon_0}$. The unknown coefficient functions $A(k_z)$ and $B(k_z)$ can be solved based on boundary conditions at $\rho = b$, where

$$E_{\phi 1} = E_{\phi 2}, \tag{4a}$$

$$H_{z1} - H_{z2} = J_s, \tag{4b}$$

$$J_s = I_0\delta\left(z\right) = \frac{I_0}{2\pi}\int_{-\infty}^{\infty} e^{-jk_z z} dk_z, \tag{4c}$$

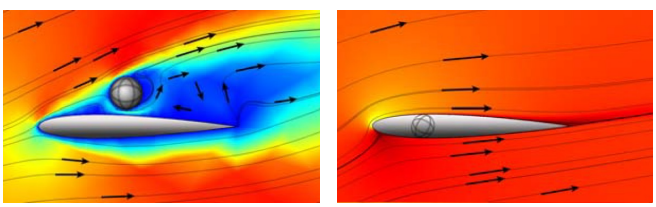

(a) AUV with a conventional triaxial antenna (b) AUV with geometry-conformal antenna

Fig. 1. Velocity fields of flows around an AUV

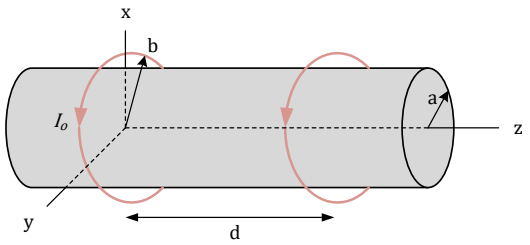

Fig. 2. The equivalent model of geometry-conformal antenna

Furthermore, the unknown coefficient function $C(k_z)$ can be solved based on boundary conditions at $\rho = a$, where

$$\frac{E_\phi}{H_z} = -Z_s. \tag{5}$$

Finally, the electric and magnetic field components can be derived by

$$\begin{cases} E_\rho = -\frac{1}{\varepsilon\rho}\frac{\partial F_z}{\partial \phi}, \\ E_\phi = -\frac{1}{\varepsilon}\frac{\partial F_z}{\partial \rho}, \\ E_z = 0, \end{cases} \tag{6}$$

$$\begin{cases} H_\rho = \frac{1}{j\omega\mu\varepsilon}\frac{\partial^2 F_z}{\partial\rho\partial z}, \\ H_\phi = \frac{1}{j\omega\mu\varepsilon\rho}\frac{\partial^2 F_z}{\partial\phi\partial z}, \\ H_z = \frac{1}{j\omega\mu\varepsilon}\left(\frac{\partial^2}{\partial z^2} + k^2\right) F_z, \end{cases} \tag{7}$$

The induced voltage in the receiver can be estimated by doing a circular integral of E_ϕ, which is

$$V_2 = -(2\pi b) E_\phi^{(1)}(d, b), \tag{8}$$

where V_2 is the open-circuit voltage induced at the terminals of receiver coil 2, and $E_\phi^{(1)}(d, b)$ is the electric field produced by the transmitter coil 1 at $z = d$ and $\rho = b$.

C. FEM Simulation and Numerical Analysis

In this subsection, we intend to quantify the influence of the metallic surface on the MI signal strength received by the geometry-conformal antenna. The induced voltage on the receiver coil was measured after applying a harmonic current with $I_0 = 0.1$A and $f = 1$MHz on the transmitter coil as shown in Fig.2. The pipe with radius $a = 2$ inch is assumed to be a perfect electric conductor, which corresponds to $Z_s = 0$. The results under different distance d were obtained through simulations as well as numerical analysis based on the mathematical model derived in subsection II-A.

In Fig. 3, we show the induced voltage in the receiver coil for different gap (gap $= \frac{b-a}{2}$) configurations. The theoretical curves match the simulation very well. The induced voltage attenuates faster as the gap getting smaller. The reasons are twofold. The magnetic field generated by the transmitter coil will be much weaker as the the gap gets smaller, which results in a smaller B. Also, the smaller gap on the receiver side means that there is a much smaller area S for the receiver coil. Since $V_2 = S\frac{dB}{dt}$, the received signal will get smaller.

III. Ferrite Impact Analysis

In this section, we show that the intensity of MI signal in geometry-conformal antennas can be significantly enhanced by applying ferrite materials between the metallic surface and the coil. The effect of different permeabilities and coverage angles of ferrite materials on MI signal strength are simulated by COMSOL Multiphysics simulation tools.

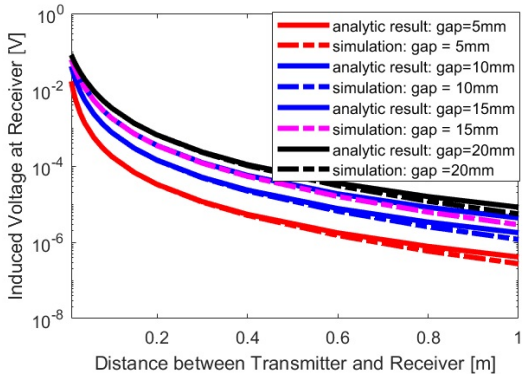

Fig. 3. MI signal strength of geometry-conformal antenna

A. The Impact on the Transmitter Side

As illustrated in section II, on the transmitter side, the metallic surface will generate opposite image currents to cancel out the magnetic field that generated by the excitation current. In this subsection, we will demonstrate that by applying ferrite materials between the coil and metallic surface, the magnetic field can be significantly enhanced. Due to the complex boundary conditions, it is hard to derive a close form expression of the generated field. But the enforcement effect of ferrite materials can be easily observed through COMSOL simulations, as shown in Fig.4.

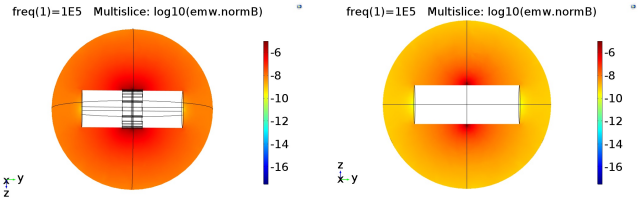

(a) With ferrite (b) Without ferrite

Fig. 4. Magnetic field strength of conformal antenna with and without ferrite materials. Dark color means strong intensity

B. The Impact of Ferrite Permeability

As for MI system, the amplitude of the induced voltage on the receiver antenna is proportional to the magnetic flux

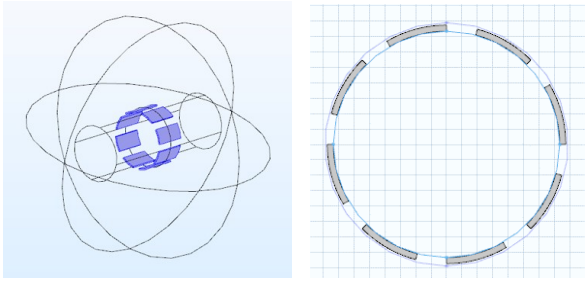

(a) Conformal antenna model (b) Ferrite arrangement

Fig. 5. Ferrite assisted geometry-conformal MI antenna model

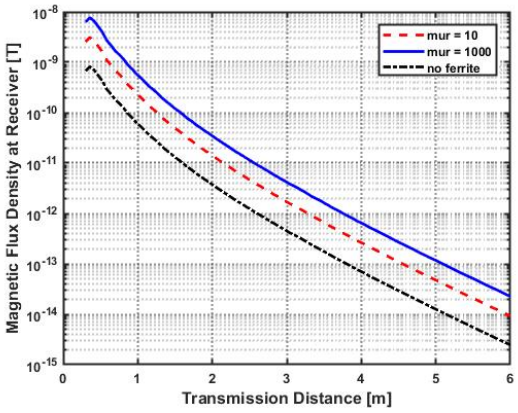

(a) Magnetic field strength

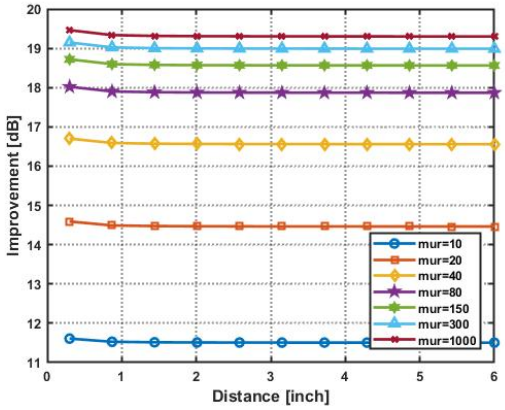

(b) Improvement comparison

Fig. 6. The impact of ferrite permeability to the magnetic field

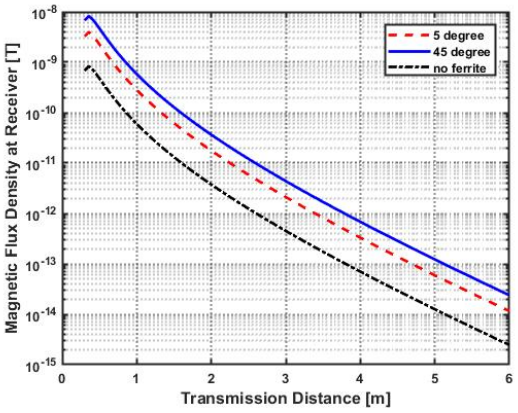

(a) Magnetic field strength

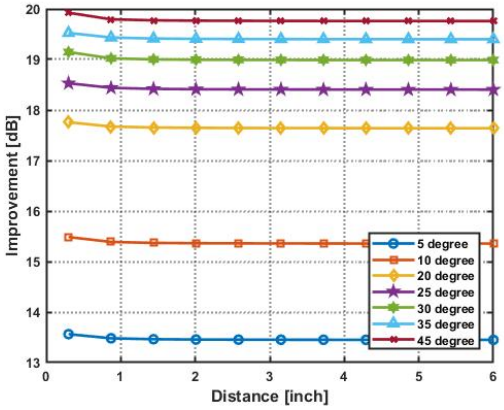

(b) Improvement comparison

Fig. 7. The impact of ferrite coverage ratio to the magnetic field

density B generated by the transmitting coil antenna. Based on the constitutive equation of magnetic materials that $B = \mu H$, the stronger MI signal would be expected if the ferrite material with higher permeability is used. The quantitative analysis were carried out through COMSOL simulations. The simulation model of ferrite assisted geometry-conformal antenna is shown in Fig.5(a). By varying the relative permeability of ferrite materials, different magnetic flux densities around the transmitting coil can be measured. The overall simulation parameters are summarized in Table I.

TABLE I
SIMULATION PARAMETERS

Parameter	Value	Description
f	100 kHz	Operation frequency
a	2.25 inch	Radius of pipe
b	2.5 inch	Radius of coil
l	20 inch	Length of the pipe
N	1	Number of turns
I_1	0.1 A	Excitation current

In Fig. 6, we show the simulation results along the co-axle direction. Overall, the higher ferrite permeability results in a stronger magnetic field. More than 18dB antenna gain can be expected if the ferrite materials with relative permeability higher than 100 is applied.

C. The Impact of Ferrite Coverage Angle

Beside the ferrite permeability, the ferrite coverage area will also impact the strength of the magnetic field generated by the transmitting coil antenna. Here, we refer to an angle to present the ferrite coverage area as shown in Fig. 5(b). Eight pieces of ferrite sheet were equally attached on an cylindrical surface. Hence, The ferrite coverage ratio can be measured by an angle (e.g. 45 degree represents fully coverage).

In Fig. 7, the magnetic field intensity is measured under different coverage angles from 5 to 45 degrees. Here, the permeability of the ferrite materials is set to 300. It is shown that, the full coverage can achieve the best antenna gain, nearly 20db enhancement compared to the situation without ferrite materials. But for economical considerations, 25 degree is a good choice, which can achieve more than 18db improvement with only 55% ferrite material usage.

IV. MI Channel Capacity for Ferrite Assisted Geometry-Conformal Antennas

In this section, we firstly illustrate how to estimate the channel capacity based on the field intensity detected on the receiver coil antenna for MI wireless communication systems. Then a simulation model with two ferrite assisted geometry-conformal antennas is established in COMSOL simulation environments to investigate the MI signal attenuation. The simulation results in the air are verified by the experiment results. Finally, we use the simulation results in sea water to estimate the subsea MI wireless channel capacity for geometry-conformal antennas.

A. Mathematical Model for Subsea MI Channel Capacity

Based on the Shannon capacity theory, the channel capacity C can be estimated by

$$C = W \log_2(1 + SNR), \tag{9}$$

where, W is the bandwidth and SNR stands for the signal to noise ratio. In this paper, we choose $W = \frac{f}{2}$ to estimate the MI channel capacity, here f is the operating frequency.

Let us first analyze the MI signal noise in subsea environments. The ambient noise can be ignored in subsea environments thanks to the fast attenuation of EM waves in sea water. Furthermore, since the coil antenna is working on resonance conditions, the antenna has a good filter effect to the induced EM noise. Hence, the noise level is only determined by the receiver circuit design (such as voltage regulator, PCB layout, etc), which can be regarded as an constant V_n.

The induced voltage V_2 can be calculated following Faraday's law or by doing a circular integral of electric field on the receiver side,

$$V_2 = -N\frac{d\Phi}{dt}, \tag{10}$$

or

$$V_2 = N \oint bE_\phi d\phi, \tag{11}$$

where N is number of turns, b is the coil radius, E_ϕ is the azimuth component of electric field under cylindrical coordinates, and $\Phi = \vec{B} \cdot \vec{A}$ is the magnetic flux, where B is the flux density and A is the effective area of the receiving coil.

The receiver coil antenna will be working on resonance conditions. So the received voltage is

$$V_r = QV_2, \tag{12}$$

where Q is the quality factor of the receiving coil.

Finally, the SNR in Eq. 9 can be estimated as

$$SNR = \left(\frac{V_r}{V_n}\right)^2. \tag{13}$$

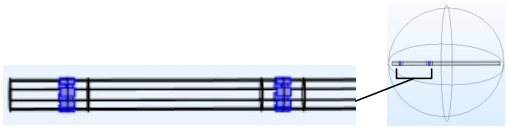

Fig. 8. Simulation model of MI wireless communication system

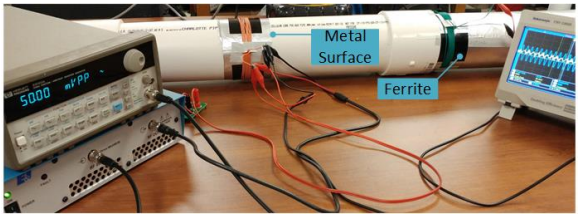

Fig. 9. The experiment setup

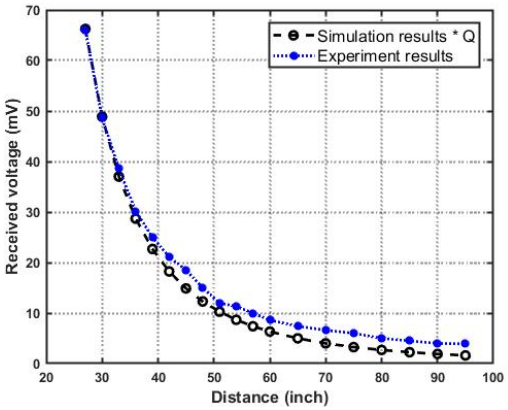

Fig. 10. The received voltage amplitude vs distance in the air. Q is the quality factor of the receiving antenna

B. Simulation Model and Experimental Verification

The COMSOL simulation model of a MI wireless communication system with two ferrite assisted geometry-conformal antennas is shown in Fig. 8. In order to verify the simulation results, the equivalent experiment testbed was set up in the air as shown in Fig. 9. The simulation and experimental parameters are the same value as in Table. I except that $N = 10$, $I \approx 0.023$A and $f = 550$kHz. The quality factor of the coil antenna is $Q \approx 100$.

Consider the simulation only measured the induced voltage V_2 on the receiver antenna. But the testing coil works under resonance conditions. As stated in Eq.12, there should be a 100 (since $Q = 100$) times mismatch between the simulation and experiment results. According to the comparisons given in Fig.10, the simulation results show a close match with the experimental results, which give us confidence to estimate the subsea MI channel capacity based on this simulation model.

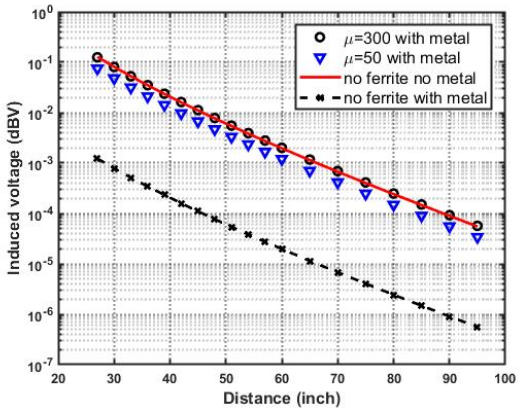

Fig. 11. MI signal intensity of different coil antenna settings with $I_1 = 0.1$A, $f = 550$kHz, $N = 10$ and coil radius $b = 2.5$inch in seawater. μ is the relative permeability of the ferrite materials.

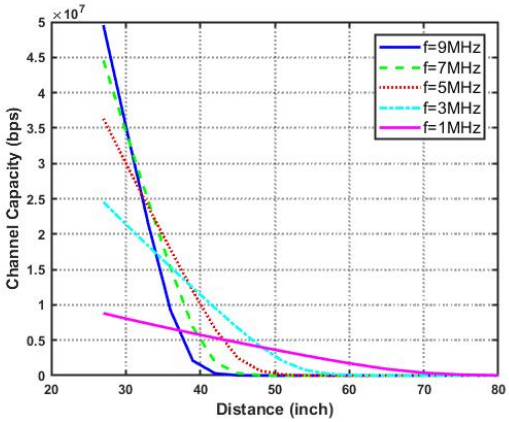

Fig. 12. Subsea MI channel capacity supported by ferrite assisted geometry-conformal antennas under different operation frequencies with $I_1 = 0.1$A, $N = 10$ and coil radius $b = 2.5$inch.

C. Subsea MI Channel Capacity Estimation

By changing the medium from the air to sea water in COMSOL, we obtain the subsea MI signal propagation model. To estimate the channel capacity, we assume that the noise power is -80dbm which follows the enhanced sensitivity level of bluetooth. Once the induced voltage was obtained, we can estimate the subsea MI channel capacity based on Eq. 9.

In Fig. 11, the MI signal intensity for different MI antenna settings are compared. The red curve represents the results for a normal two coil antenna systems and the propagation medium is the pure sea water. The dash-dot curve is the result for geometry-conformal antennas. It is shown that the metallic surface weaken the signal significantly. After applying the ferrite materials, the intensity of MI signal is enhanced to the same level as a normal antenna. The enhanced effect is depending on the permeability of ferrite materials. The higher permeability would have better enhance performances as shown in the circle and triangle plot.

Finally, we study the MI channel capacity that can be achieved by the proposed ferrite assisted geometry-conformal antenna. In Fig. 12, the channel capacity is plotted as a function of transmission distances under different operating frequencies. It shows that the higher operating frequency can achieve much higher channel capacity. However, the signal with higher frequency will also attenuates much faster. Overall, up to several Mbps data rate can be achieved for our novel ferrite assisted geometry-conformal antenna design within the near region for submarine devices with a metallic body like AUVs.

V. Conclusion

Subsea environments are extremely challenging for wireless communications. However, MI technology is suitable for short range (few meters), high speed(few Mbps) and high power efficient subsea wireless communications. By regarding that metals can shield the magnetic field, the ferrite assisted geometry-conformal wireless antenna proposed in this paper is a good solution to realize MI wireless communications between different kinds of submarine devices such as AUVs, sensors and pipelines.

References

[1] X. Che, I. Wells, G. Dickers, P. Kear, and X. Gong, "Re-evaluation of rf electromagnetic communication in underwater sensor networks," *IEEE Communications Magazine*, vol. 48, no. 12, pp. 143–151, 2010.

[2] M. Stojanovic and J. Preisig, "Underwater acoustic communication channels: Propagation models and statistical characterization," *IEEE communications magazine*, vol. 47, no. 1, pp. 84–89, 2009.

[3] Y. Li, Y. Zhang, W. Li, and T. Jiang, "Marine wireless big data: Efficient transmission, related applications, and challenges," *IEEE Wireless Communications*, vol. 25, no. 1, pp. 19–25, February 2018.

[4] Z. Sun and I. F. Akyildiz, "Magnetic induction communications for wireless underground sensor networks," *IEEE Transactions on Antennas and Propagation*, vol. 58, no. 7, pp. 2426–2435, 2010.

[5] I. F. Akyildiz, P. Wang, and Z. Sun, "Realizing underwater communication through magnetic induction," *IEEE Communications Magazine*, vol. 53, no. 11, pp. 42–48, 2015.

[6] M. C. Domingo, "Magnetic induction for underwater wireless communication networks," *IEEE Transactions on Antennas and Propagation*, vol. 60, no. 6, pp. 2929–2939, 2012.

[7] B. Gulbahar and O. B. Akan, "A communication theoretical modeling and analysis of underwater magneto-inductive wireless channels," *IEEE Transactions on Wireless Communications*, vol. 11, no. 9, pp. 3326–3334, 2012.

[8] D. Wei, L. Yan, X. Li, Y. Sun, D. Yuan, J. Chen, and M. Pan, "Exploiting magnetic field analysis to characterize mi wireless communications in subsea environments," in *2018 International Conference on Computing, Networking and Communications (ICNC)*. IEEE, 2018, pp. 805–809.

[9] H. Guo, Z. Sun, and P. Wang, "Channel modeling of mi underwater communication using tri-directional coil antenna," in *Global Communications Conference , 2015 IEEE*. IEEE, 2015, pp. 1–6.

[10] N. Ahmed, Y. R. Zheng, and D. Pommerenke, "Effects of metal structures on magneto-inductive coupled coils," in *Underwater Communications and Networking Conference (UComms), 2016 IEEE Third*. IEEE, 2016, pp. 1–4.

[11] X. Xin, D. R. Jackson, and J. Chen, "Wireless power transfer along oil pipe using ferrite materials," *IEEE Transactions on Magnetics*, vol. 53, no. 3, pp. 1–5, 2017.